International Journal of Analysis and Applications

Analytical Solutions to the Fractional Zhiber-Shabat Equation Using the Unified Method

Ahmed M. A. Adam[1], Elzain A. E. Gumma[1], Ali Satty[1], Mohyaldein Salih[1], Zakariya M. S. Mohammed[1,2], Gamal Saad Mohamed Khamis[3], Omer M. A. Hamed[4], Abaker A. Hassaballa[1,2,*]

[1]*Department of Mathematics, College of Science, Northern Border University, Arar, Saudi Arabia*
[2]*Center for Scientific Research and Entrepreneurship, Northern Border University, Arar, Saudi Arabia*
[3]*Department of Computer Science, College of Science, Northern Border University, Arar, Saudi Arabia*
[4]*Department of Finance and Insurance, College of Business Administration, Northern Border University, Arar, Saudi Arabia*

**Corresponding author:* abakerh@gmail.com

ABSTRACT. In this study, exact solutions of the conformable fractional Zhiber–Shabat (Z–S) equation have been investigated using the unified method. The primary objective is to apply this method to derive analytical solutions to the fractional Z–S equation. Graphical visualizations of selected solutions are presented to demonstrate the influence of the fractional order on wave dynamics. The results confirm the reliability and effectiveness of the unified method in solving the Z–S equation.

1. Introduction

The investigation of exact solutions for nonlinear partial differential equations (NLPDEs) plays a crucial role in deepening our understanding of numerous physical processes. Over time, a variety of analytical techniques have been developed to derive such solutions, including the homogeneous balance method [1], Hirota's bilinear method [2], the Tanh method [3], the inverse scattering transform [4], the extended F-expansion method [5], the exp-function method [6], the (G'/G)-expansion method [7], the variational iteration transform method [8], and the optimized

Received Jun. 23, 2025

2020 Mathematics Subject Classification. 35R11.

Key words and phrases. nonlinear fractional partial differential equations; conformable fractional derivative; unified method; traveling wave solutions; Zhiber-Shabat equation.

https://doi.org/10.28924/2291-8639-23-2025-230

ISSN: 2291-8639

decomposition method [9]. More recently, increased attention has been directed toward nonlinear fractional partial differential equations (NLFPDEs), owing to their capacity to incorporate memory and non-local effects. These equations have found widespread application across various disciplines, including mathematical modeling, physics, engineering, biological systems, and economic analysis [10–13].

The Zhiber-Shabat Equation [14] is written as follows

$$w_{xt} + ae^{w} + be^{-w} + ce^{-2w} = 0 \tag{1.1}$$

where w is a function in x and t, and $a, b, c \in \mathbb{R}$.

The Z-S equation plays a significant role in various branches of science, including mathematical biology, fluid dynamics, solid-state physics, nonlinear optics, chemical kinetics, plasma physics, crystal dislocation theory, kink dynamics, and quantum field theory [14]. Due to its wide range of applications, the Z-S equation has been the subject of extensive research, and numerous analytical techniques have been employed to obtain its solutions. These include the Tanh method [14], bifurcation theory [15], the Hermite transform in conjunction with the homogeneous balance method [16], the $\exp(-\phi(\xi)$-expansion method [17], the Jacobi elliptic function method [18], the (1/G′)-expansion and (G′/G, 1/G)-expansion methods [19], the improved F-expansion method [20], the rational hyperbolic function method [21], the (G'/G)-expansion method [22], the modified Tanh–Coth method [23], Lie symmetry analysis coupled with the extended direct algebraic method [24], modified Kudryashov and extended simple equation methods [25] and Sardar sub-equation method [26].

The conformable fractional Z-S equation is given by

$$D_{xt}^{2\alpha} w + ae^{w} + be^{-w} + ce^{-2w} = 0 \tag{1.2}$$

where D_x^{α} denotes the CFD with respect to x and $D_{xt}^{2\alpha} = D_t^{\alpha}(D_x^{\alpha})$.

Numerous formulations of fractional derivatives have been developed to address diverse modeling requirements. Among the most prominent are the conformable fractional derivative, Caputo derivative, Riemann–Liouville and its modified form, as well as the Hilfer, Riesz, and Atangana derivatives [27–30].

According to [30], the conformable fractional derivative (CFD) of order α with respect to the independent variable z is defined as follows

$$D^{\alpha} g(z) = \lim_{\delta \to 0} \frac{g\left(z + \delta z^{1-\alpha}\right) - g(z)}{\delta}, \forall z > 0, \alpha \in (0,1]$$

$$g^{(\alpha)}(0) = \lim_{z \to 0^{+}} g^{(\alpha)}(z)$$

Suppose that g and h are α −differentiable functions at $z > 0$. In the special case $\alpha = 1$, the CFD is reduced to the classical integer derivative. The CFD possesses the following properties:

$$D^{\alpha} z^{m} = m z^{m-\alpha}, m \in R \tag{I}$$

$$D^{\alpha} C = 0. \tag{II}$$

$D^{\alpha}(Ag + Bh) = AD^{\alpha}g + BD^{\alpha}h$ (III)

$D^{\alpha}(gh) = gD^{\alpha}h + hD^{\alpha}g$ (IV)

$D^{\alpha}\left(\frac{g}{h}\right) = \frac{hD^{\alpha}g - gD^{\alpha}h}{h^2}$ (V)

$D^{\alpha}h(z) = z^{1-\alpha}\frac{dh}{dz}$ (VI)

$D^{\alpha}g(h) = z^{1-\alpha}h'(z)g'(h(z))$, (VII)

where A, B, and C are constants. The proofs of these properties are given in [30].

The CFD offers several notable advantages [30, 31], it adheres to the fundamental principles and properties of the classical derivative, it is adaptable to both exact and numerical solutions of fractional differential equations, and it extends classical integral transforms, including the Laplace and Sumudu transforms. This study focuses on applying the unified method to obtain solutions of the conformable fractional Z-S equation. The unified method is a robust analytical technique for deriving closed-form solutions to both NLPDEs and NLFPDEs [32–37]. The primary aim of this study is to demonstrate the effectiveness of the unified method in obtaining exact solutions for the conformable fractional Z-S equation. This method offers several advantages, such as integrating multiple solution techniques into a simplified framework, thereby enhancing efficiency and comprehensiveness without adding unnecessary complexity [33]. While previous approaches [14-23] have been employed to solve the nonlinear Z-S equation, none have extensively applied the unified method to this specific equation. Therefore, the novelty of this work lies in the application of the unified method to the fractional Z-S equation. This topic has not been thoroughly explored in the existing literature. The paper is organized as follows: Section 2 describes the unified method. Section 3 applies the method to solve the fractional Z-S equation. Section 4 provides graphical illustrations. Finally, Section 5 concludes the study.

2. Description of the unified method

The steps of the method are as follows [32]:

***Step* 1:** Consider a NLFPDE of the form:

$F(w, D_t^{\alpha}w, D_x^{\alpha}w, D_{xt}^{2\alpha}w, D_t^{2\alpha}w, D_x^{2\alpha}w, \dots) = 0,$ (2.1)

where w is the unknown function of spatial coordinate x and temporal variable t. The solutions to Eq. (2.1) are derived by applying the following traveling wave transformation

$w(x,t) = W(\eta)$, where $\eta = (kx^{\alpha} - \omega t^{\alpha})/\alpha,$ (2.2)

Eq. (2.1) is reduced to an ODE:

$F(W, W', W'', W''', \dots) = 0,$ (2.3)

where $W' = \frac{dW}{d\eta}$.

***Step* 2:** The solution Eq. (2.3) is assumed to be of the form:

$W(\eta) = \rho_0 + \sum_{j=1}^{N}[\rho_j\psi^j + \mu_j\psi^{-j}],$ (2.4)

where $\psi = \psi(\eta)$ satisfies the Riccati equation

$$\psi' = \xi + \psi^2(\eta), \tag{2.5}$$

and ξ is a constant. The positive integer N is obtained by equating the highest-order derivatives and the nonlinear terms of the highest degree in Eq. (2.3). Additionally, ρ_j, μ_j and ρ_0 are coefficients that need to be determined. The following three families give the general solutions of Eq. (2.5):

Family 1. If $\xi < 0$, the solutions are

$$\psi(\eta) = \begin{cases} \psi_1 = \frac{\sqrt{-(\beta^2+\gamma^2)\xi}-\beta\sqrt{-\xi}\cosh\left(2\sqrt{-\xi}(\eta+\eta_0)\right)}{\beta\sinh\left(2\sqrt{-\xi}(\eta+\eta_0)\right)+\gamma} \\ \psi_2 = \frac{-\sqrt{-(\beta^2+\gamma^2)\xi}-\beta\sqrt{-\xi}\cosh\left(2\sqrt{-\xi}(\eta+\eta_0)\right)}{\beta\sinh\left(2\sqrt{-\xi}(\eta+\eta_0)\right)+\gamma} \\ \psi_3 = \sqrt{-\xi} + \frac{-2\beta\sqrt{-\xi}}{\beta+\cosh\left(2\sqrt{-\xi}(\eta+\eta_0)\right)-\sinh\left(2\sqrt{-\xi}(\eta+\eta_0)\right)} \\ \psi_4 = -\sqrt{-\xi} + \frac{2\beta\sqrt{-\xi}}{\beta+\cosh\left(2\sqrt{-\xi}(\eta+\eta_0)\right)+\sinh\left(2\sqrt{-\xi}(\eta+\eta_0)\right)} \end{cases} \tag{2.6}$$

Family 2. If $\xi > 0$, the solutions are

$$\psi(\eta) = \begin{cases} \psi_5 = \frac{\sqrt{(\beta^2-\gamma^2)\xi}-\beta\sqrt{\xi}\cos\left(2\sqrt{\xi}(\eta+\eta_0)\right)}{\beta\sin\left(2\sqrt{\xi}(\eta+\eta_0)\right)+\gamma} \\ \psi_6 = \frac{-\sqrt{(\beta^2-\gamma^2)\xi}-\beta\sqrt{\xi}\cos\left(2\sqrt{\xi}(\eta+\eta_0)\right)}{\beta\sin\left(2\sqrt{\xi}(\eta+\eta_0)\right)+\gamma} \\ \psi_7 = i\sqrt{\xi} + \frac{-2\beta i\sqrt{\xi}}{\beta+\cos\left(2\sqrt{\xi}(\eta+\eta_0)\right)-i\sin\left(2\sqrt{\xi}(\eta+\eta_0)\right)} \\ \psi_8 = -i\sqrt{\xi} + \frac{2\beta i\sqrt{\xi}}{\beta+\cos\left(2\sqrt{\xi}(\eta+\eta_0)\right)+i\sin\left(2\sqrt{\xi}(\eta+\eta_0)\right)} \end{cases} \tag{2.7}$$

Family 3. If $\xi = 0$, the solution is

$$\psi(\eta) = -\frac{1}{\eta+\eta_0}, \tag{2.8}$$

where $\beta \neq 0$ and $\gamma, \eta_0 \in \mathbb{R}$.

***Step* 3:** Substituting Eqs. (2.4) and (2.5) in Eq. (2.3), and equating the coefficients of like powers of ψ to zero yields a system of algebraic equations. This system is then solved using Maple to determine the values of ρ_j, μ_j, k, ω, and ρ_0. These values are then used along with the general solutions of Eq. (2.5) to obtain the exact solutions of Eq. (2.1).

3. Application

In this section, the unified method is utilized to derive exact solutions for Eq. (1.2). According to Painlevé transformation $u = e^w$ and the traveling wave transformation, Eq. (1.2) becomes

$$-k\omega(WW'' - W'^2) + aW^3 + bW + c = 0. \tag{3.1}$$

If we set $a = 1$, $b = -\frac{3}{2}$ and $c = \frac{1}{2}$, we get

$$-k\omega(WW'' - W'^2) + W^3 - \frac{3}{2}W + \frac{1}{2} = 0. \tag{3.2}$$

Balancing WW'' with W^3 gives $N = 2$. Thus, the solutions of Eq. (3.2) can be expressed in the form

$$W(\eta) = \rho_0 + \rho_1\psi + \rho_2\psi^2 + \mu_1\psi^{-1} + \mu_2\psi^{-2}. \tag{3.3}$$

Inserting Eqs. (3.3) and (2.5) into Eq. (3.2) and equating the coefficients of the powers of ψ to zero produces a system of algebraic equations. This system is then solved with Maple to obtain the following:

Set 1: $\rho_1 = \rho_2 = \mu_1 = 0,\ k = k,\ \rho_0 = \frac{1}{4},\ \mu_2 = -\frac{3\xi}{4},\ \omega = -\frac{3}{8k\xi}$.

Set 2: $\rho_1 = \mu_1 = \mu_2 = 0,\ k = k,\ \rho_0 = \frac{1}{4},\ \rho_2 = -\frac{3}{4\xi},\ \omega = -\frac{3}{8k\xi}$.

Set 3: $\rho_1 = \rho_2 = \mu_1 = 0,\ k = k,\ \rho_0 = 1 + \frac{\sqrt{3}}{2},\ \mu_2 = \frac{3\xi}{2},\ \omega = \frac{3}{4k\xi}$.

Set 4: $\rho_1 = \rho_2 = \mu_1 = 0, c\ k = k,\ \rho_0 = 1 - \frac{\sqrt{3}}{2},\ \mu_2 = \frac{3\xi}{2},\ \omega = \frac{3}{4k\xi}$.

Set 5: $\rho_1 = \mu_1 = \mu_2 = 0,\ k = k,\ \rho_0 = \rho_0 = 1 + \frac{\sqrt{3}}{2},\ \rho_2 = \frac{3}{2\xi},\ \omega = \frac{3}{4k\xi}$.

Set 6: $\rho_1 = \mu_1 = \mu_2 = 0,\ k = k,\ \rho_0 = \rho_0 = 1 - \frac{\sqrt{3}}{2},\ \rho_2 = \frac{3}{2\xi},\ \omega = \frac{3}{4k\xi}$.

Set 7: $\rho_1 = \mu_1 = 0,\ k = k,\ \rho_0 = \frac{5}{8},\ \rho_2 = -\frac{3}{16\xi},\ \mu_2 = -\frac{3\xi}{16},\ \omega = -\frac{3}{32k\xi}$.

Set 8: $\rho_1 = \mu_1 = 0,\ k = k,\ \rho_0 = \frac{1}{4} + \frac{\sqrt{3}}{2},\ \rho_2 = \frac{3}{8\xi},\ \mu_2 = \frac{3\xi}{8},\ \omega = \frac{3}{16k\xi}$.

Set 9: $\rho_1 = \mu_1 = 0,\ k = k,\ \rho_0 = \frac{1}{4} - \frac{\sqrt{3}}{2},\ \rho_2 = \frac{3}{8\xi},\ \mu_2 = \frac{3\xi}{8},\ \omega = \frac{3}{16k\xi}$.

Using the above sets, family 1 and family 3, we obtain the exact hyperbolic and rational solutions of the conformable fractional Z-S equation as follows:

For set 1:

$$w_1(x,t) = ln\left(\frac{1}{4} - \frac{3\xi}{4}\left[\frac{\beta\sinh\left(2\sqrt{-\xi}(\eta+\eta_0)\right)+\gamma}{\pm\sqrt{-(\beta^2+\gamma^2)\xi}-\beta\sqrt{-\xi}\cosh\left(2\sqrt{-\xi}(\eta+\eta_0)\right)}\right]^2\right),$$

$$w_2(x,t) = ln\left(\frac{1}{4} - \frac{3\xi}{4}\left[\frac{\beta+\cosh\left(2\sqrt{-\xi}(\eta+\eta_0)\right)\mp\sinh\left(2\sqrt{-\xi}(\eta+\eta_0)\right)}{\pm\sqrt{-\xi}\left(-\beta+\cosh\left(2\sqrt{-\xi}(\eta+\eta_0)\right)\mp\sinh\left(2\sqrt{-\xi}(\eta+\eta_0)\right)\right)}\right]^2\right),$$

$$w_3(x,t) = ln\left(\frac{1}{4} - \frac{3\xi}{4}\left[-\frac{1}{\eta+\eta_0}\right]^{-2}\right)$$

for set 2:

$$w_4(x,t) = ln\left(\frac{1}{4} - \frac{3}{4\xi}\left[\frac{\pm\sqrt{-(\beta^2+\gamma^2)\xi}-\beta\sqrt{-\xi}\cosh\left(2\sqrt{-\xi}(\eta+\eta_0)\right)}{\beta\sinh\left(2\sqrt{-\xi}(\eta+\eta_0)\right)+\gamma}\right]^2\right),$$

$$w_5(x,t) = ln\left(\frac{1}{4} - \frac{3}{4\xi}\left[\frac{\pm\sqrt{-\xi}\left(-\beta+\cosh\left(2\sqrt{-\xi}(\eta+\eta_0)\right)\mp\sinh\left(2\sqrt{-\xi}(\eta+\eta_0)\right)\right)}{\beta+\cosh\left(2\sqrt{-\xi}(\eta+\eta_0)\right)\mp\sinh\left(2\sqrt{-\xi}(\eta+\eta_0)\right)}\right]^2\right),$$

$$w_6(x,t) = ln\left(\frac{1}{4} - \frac{3}{4\xi}\left[-\frac{1}{\eta+\eta_0}\right]^2\right),$$

where $\eta = (kx^\alpha + \frac{3}{8k\xi}t^\alpha)/\alpha$.

For set 3:

$$w_7(x,t) = ln\left(1+\frac{\sqrt{3}}{2}+\frac{3\xi}{2}\left[\frac{\beta\sinh\left(2\sqrt{-\xi}(\eta+\eta_0)\right)+\gamma}{\pm\sqrt{-(\beta^2+\gamma^2)\xi}-\beta\sqrt{-\xi}\cosh\left(2\sqrt{-\xi}(\eta+\eta_0)\right)}\right]^2\right),$$

$$w_8(x,t) = ln\left(1+\frac{\sqrt{3}}{2}+\frac{3\xi}{2}\left[\frac{\beta+\cosh\left(2\sqrt{-\xi}(\eta+\eta_0)\right)\mp\sinh\left(2\sqrt{-\xi}(\eta+\eta_0)\right)}{\pm\sqrt{-\xi}\left(-\beta+\cosh\left(2\sqrt{-\xi}(\eta+\eta_0)\right)\mp\sinh\left(2\sqrt{-\xi}(\eta+\eta_0)\right)\right)}\right]^2\right),$$

for set 4:

$$w_9(x,t) = ln\left(1-\frac{\sqrt{3}}{2}+\frac{3\xi}{2}\left[\frac{\beta\sinh\left(2\sqrt{-\xi}(\eta+\eta_0)\right)+\gamma}{\pm\sqrt{-(\beta^2+\gamma^2)\xi}-\beta\sqrt{-\xi}\cosh\left(2\sqrt{-\xi}(\eta+\eta_0)\right)}\right]^2\right),$$

$$w_{10}(x,t) = ln\left(1-\frac{\sqrt{3}}{2}+\frac{3\xi}{2}\left[\frac{\beta+\cosh\left(2\sqrt{-\xi}(\eta+\eta_0)\right)\mp\sinh\left(2\sqrt{-\xi}(\eta+\eta_0)\right)}{\pm\sqrt{-\xi}\left(-\beta+\cosh\left(2\sqrt{-\xi}(\eta+\eta_0)\right)\mp\sinh\left(2\sqrt{-\xi}(\eta+\eta_0)\right)\right)}\right]^2\right),$$

$$w_{11}(x,t) = ln\left(1\pm\frac{\sqrt{3}}{2}+\frac{3\xi}{2}\left[-\frac{1}{\eta+\eta_0}\right]^{-2}\right),$$

for set 5:

$$w_{12}(x,t) = ln\left[1+\frac{\sqrt{3}}{2}+\frac{3}{2\xi}\left(\frac{\pm\sqrt{-(\beta^2+\gamma^2)\xi}-\beta\sqrt{-\xi}\cosh\left(2\sqrt{-\xi}(\eta+\eta_0)\right)}{\beta\sinh\left(2\sqrt{-\xi}(\eta+\eta_0)\right)+\gamma}\right)^2\right],$$

$$w_{13}(x,t) = ln\left[1+\frac{\sqrt{3}}{2}+\frac{3}{2\xi}\left(\frac{\pm\sqrt{-\xi}\left(-\beta+\cosh\left(2\sqrt{-\xi}(\eta+\eta_0)\right)\mp\sinh\left(2\sqrt{-\xi}(\eta+\eta_0)\right)\right)}{\beta+\cosh\left(2\sqrt{-\xi}(\eta+\eta_0)\right)\mp\sinh\left(2\sqrt{-\xi}(\eta+\eta_0)\right)}\right)^2\right],$$

for set 6:

$$w_{14}(x,t) = ln\left[1-\frac{\sqrt{3}}{2}+\frac{3}{2\xi}\left(\frac{\pm\sqrt{-(\beta^2+\gamma^2)\xi}-\beta\sqrt{-\xi}\cosh\left(2\sqrt{-\xi}(\eta+\eta_0)\right)}{\beta\sinh\left(2\sqrt{-\xi}(\eta+\eta_0)\right)+\gamma}\right)^2\right],$$

$$w_{15}(x,t) = ln\left[1-\frac{\sqrt{3}}{2}+\frac{3}{2\xi}\left(\frac{\pm\sqrt{-\xi}\left(-\beta+\cosh\left(2\sqrt{-\xi}(\eta+\eta_0)\right)\mp\sinh\left(2\sqrt{-\xi}(\eta+\eta_0)\right)\right)}{\beta+\cosh\left(2\sqrt{-\xi}(\eta+\eta_0)\right)\mp\sinh\left(2\sqrt{-\xi}(\eta+\eta_0)\right)}\right)^2\right],$$

$$w_{16}(x,t) = ln\left(1\pm\frac{\sqrt{3}}{2}+\frac{3}{2\xi}\left[-\frac{1}{\eta+\eta_0}\right]^2\right),$$

where $\eta = (kx^\alpha - \frac{3}{4k\xi}t^\alpha)/\alpha$.

For set 7:

$$w_{17}(x,t) = ln\left(\frac{5}{8}-\frac{3}{16\xi}\left[\frac{\pm\sqrt{-(\beta^2+\gamma^2)\xi}-\beta\sqrt{-\xi}\cosh\left(2\sqrt{-\xi}(\eta+\eta_0)\right)}{\beta\sinh\left(2\sqrt{-\xi}(\eta+\eta_0)\right)+\gamma}\right]^2 - \frac{3\xi}{16}\left[\frac{\beta\sinh\left(2\sqrt{-\xi}(\eta+\eta_0)\right)+\gamma}{\pm\sqrt{-(\beta^2+\gamma^2)\xi}-\beta\sqrt{-\xi}\cosh\left(2\sqrt{-\xi}(\eta+\eta_0)\right)}\right]^2\right),$$

$$w_{18}(x,t) = ln\left(\frac{5}{8}-\frac{3}{16\xi}\left[\frac{\pm\sqrt{-\xi}\left(-\beta+\cosh\left(2\sqrt{-\xi}(\eta+\eta_0)\right)\mp\sinh\left(2\sqrt{-\xi}(\eta+\eta_0)\right)\right)}{\beta+\cosh\left(2\sqrt{-\xi}(\eta+\eta_0)\right)\mp\sinh\left(2\sqrt{-\xi}(\eta+\eta_0)\right)}\right]^2 - \frac{3\xi}{16}\left[\frac{\beta+\cosh\left(2\sqrt{-\xi}(\eta+\eta_0)\right)\mp\sinh\left(2\sqrt{-\xi}(\eta+\eta_0)\right)}{\pm\sqrt{-\xi}\left(-\beta+\cosh\left(2\sqrt{-\xi}(\eta+\eta_0)\right)\mp\sinh\left(2\sqrt{-\xi}(\eta+\eta_0)\right)\right)}\right]^2\right),$$

$$w_{19}(x,t) = ln\left(\frac{5}{8} - \frac{3}{16\xi}\left[-\frac{1}{\eta+\eta_0}\right]^2 - \frac{3\xi}{16}\left[-\frac{1}{\eta+\eta_0}\right]^{-2}\right),$$

where $\eta = (kx^\alpha + \frac{3}{32k\xi}t^\alpha)/\alpha$.

For set 8:

$$w_{20}(x,t) = ln\left(\frac{1}{4} + \frac{\sqrt{3}}{2} + \frac{3}{8\xi}\left[\frac{\pm\sqrt{-(\beta^2+\gamma^2)\xi} - \beta\sqrt{-\xi}\cosh\left(2\sqrt{-\xi}(\eta+\eta_0)\right)}{\beta\sinh\left(2\sqrt{-\xi}(\eta+\eta_0)\right)+\gamma}\right]^2 + \frac{3\xi}{8}\left[\frac{\beta\sinh\left(2\sqrt{-\xi}(\eta+\eta_0)\right)+\gamma}{\pm\sqrt{-(\beta^2+\gamma^2)\xi} - \beta\sqrt{-\xi}\cosh\left(2\sqrt{-\xi}(\eta+\eta_0)\right)}\right]^2\right),$$

$$w_{21}(x,t) = ln\left(\frac{1}{4} + \frac{\sqrt{3}}{2} + \frac{3}{8\xi}\left[\frac{\pm\sqrt{-\xi}\left(-\beta+\cosh\left(2\sqrt{-\xi}(\eta+\eta_0)\right)\mp\sinh\left(2\sqrt{-\xi}(\eta+\eta_0)\right)\right)}{\beta+\cosh\left(2\sqrt{-\xi}(\eta+\eta_0)\right)\mp\sinh\left(2\sqrt{-\xi}(\eta+\eta_0)\right)}\right]^2 + \frac{3\xi}{8}\left[\frac{\beta+\cosh\left(2\sqrt{-\xi}(\eta+\eta_0)\right)\mp\sinh\left(2\sqrt{-\xi}(\eta+\eta_0)\right)}{\pm\sqrt{-\xi}\left(-\beta+\cosh\left(2\sqrt{-\xi}(\eta+\eta_0)\right)\mp\sinh\left(2\sqrt{-\xi}(\eta+\eta_0)\right)\right)}\right]^2\right),$$

for set 9:

$$w_{22}(x,t) = ln\left(\frac{1}{4} - \frac{\sqrt{3}}{2} + \frac{3}{8\xi}\left[\frac{\pm\sqrt{-(\beta^2+\gamma^2)\xi} - \beta\sqrt{-\xi}\cosh\left(2\sqrt{-\xi}(\eta+\eta_0)\right)}{\beta\sinh\left(2\sqrt{-\xi}(\eta+\eta_0)\right)+\gamma}\right]^2 + \frac{3\xi}{8}\left[\frac{\beta\sinh\left(2\sqrt{-\xi}(\eta+\eta_0)\right)+\gamma}{\pm\sqrt{-(\beta^2+\gamma^2)\xi} - \beta\sqrt{-\xi}\cosh\left(2\sqrt{-\xi}(\eta+\eta_0)\right)}\right]^2\right),$$

$$w_{23}(x,t) = ln\left(\frac{1}{4} - \frac{\sqrt{3}}{2} + \frac{3}{8\xi}\left[\frac{\pm\sqrt{-\xi}\left(-\beta+\cosh\left(2\sqrt{-\xi}(\eta+\eta_0)\right)\mp\sinh\left(2\sqrt{-\xi}(\eta+\eta_0)\right)\right)}{\beta+\cosh\left(2\sqrt{-\xi}(\eta+\eta_0)\right)\mp\sinh\left(2\sqrt{-\xi}(\eta+\eta_0)\right)}\right]^2 + \frac{3\xi}{8}\left[\frac{\beta+\cosh\left(2\sqrt{-\xi}(\eta+\eta_0)\right)\mp\sinh\left(2\sqrt{-\xi}(\eta+\eta_0)\right)}{\pm\sqrt{-\xi}\left(-\beta+\cosh\left(2\sqrt{-\xi}(\eta+\eta_0)\right)\mp\sinh\left(2\sqrt{-\xi}(\eta+\eta_0)\right)\right)}\right]^2\right),$$

$$w_{24}(x,t) = ln\left(\frac{1}{4} \pm \frac{\sqrt{3}}{2} + \frac{3}{8\xi}\left[-\frac{1}{\eta+\eta_0}\right]^2 + \frac{3\xi}{8}\left[-\frac{1}{\eta+\eta_0}\right]^{-2}\right),$$

where $\eta = (kx^\alpha - \frac{3}{16k\xi}t^\alpha)/\alpha$.

Similarly, by employing the same approach, we can derive numerous trigonometric solutions to the conformable fractional Z-S equation. This can be achieved by utilizing family 2, as shown in Eq. (2.7). For simplicity, only a few trigonometric solutions are presented below:

For set 1: we obtain

$$w_{25}(x,t) = ln\left(\frac{1}{4} - \frac{3\xi}{4}\left[\frac{\beta\sin\left(2\sqrt{\xi}(\eta+\eta_0)\right)+\gamma}{\pm\sqrt{(\beta^2-\gamma^2)\xi} - \beta\sqrt{\xi}\cos\left(2\sqrt{\xi}(\eta+\eta_0)\right)}\right]^2\right),$$

where $\eta = (kx^\alpha + \frac{3}{8k\xi}t^\alpha)/\alpha$.

For set 5: we get

$$w_{26}(x,t) = ln\left(1 + \frac{\sqrt{3}}{2} + \frac{3}{2\xi}\left[\frac{\mp i\sqrt{\xi}\left(\beta-\cos\left(2\sqrt{\xi}(\eta+\eta_0)\right)\pm i\sin\left(2\sqrt{\xi}(\eta+\eta_0)\right)\right)}{\beta+\cos\left(2\sqrt{\xi}(\eta+\eta_0)\right)\mp i\sin\left(2\sqrt{\xi}(\eta+\eta_0)\right)}\right]^2\right),$$

where $\eta = (kx^{\alpha} - \frac{3}{4k\xi}t^{\alpha})/\alpha$.

4. Graphical illustration

This section presents a graphical visualization of the conformable fractional Z-S equation to investigate the effect of changing the fractional order on the solutions $w_1(x,t)$, $w_{25}(x,t)$ and $w_{26}(x,t)$. The analysis is managed by applying different parameter values within the domains $0 \le x,t \le 10$. The 3D plots for fractional orders order $\alpha = 0.5, 0.8, 1$ are presented in panels (a)-(c), whereas panel (d) provides corresponding 2D visualization. The solution $w_{16}(x,t)$ is examined over the domain $-10 \le x \le 10$, $0 \le t \le 10$. The solutions take the form of hyperbolic, trigonometric, and rational functions in various wave shapes, including bright solitons, periodic structures, shock waves, and singular-dark solitons.

Figure 1: Panels (a-c) depict 3D plots presenting bright wave soliton solutions of $w_1(x,t)$ with parameters $k = \beta = \gamma = 1$, $\eta_0 = \xi = -1$ and fractional order $\alpha = 0.5, 0.8, 1$, respectively. In panel (a), the surface exhibits highly irregular and steep growth near the upper right region. In panel (b), although the sharp growth persists, the amplitude and steepness are moderately reduced compared to panel (a). Panel (c) presents the smoothest and most stable surface among the three, with a more uniform and less erratic peak, suggesting the presence of a higher fractional order. Panel (d) presents 2D plots at time $t = 1$, $0 \le x \le 5$ with the same parameters. The 2D plots of $w_1(x,y)$ demonstrates how the fractional order affects the singularity and peak intensity of the solution. As α decreases from 1 to 0.5, the peak becomes sharper and shifts slightly to the left.

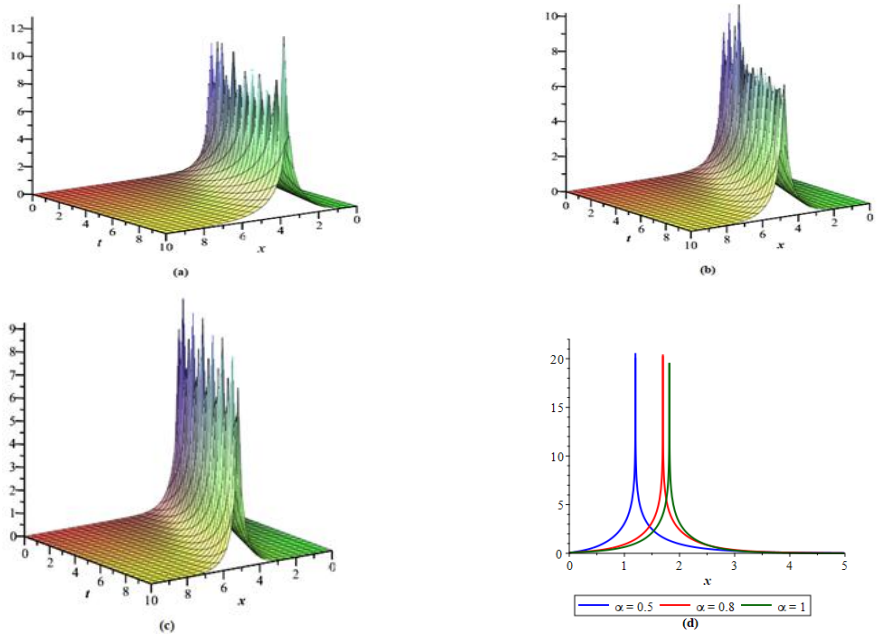

Figure 1. Behavior of wave soliton solutions: 3D and 2D visualizations of $w_1(x,y,t)$

Figure 2: Panels (a-c) depict 3D plots that display periodic solutions of $w_{25}(x,t)$ over the intervals $0 \le x,t \le 10$, with parameters $k = \beta = \eta_0 = 1, \gamma = 0, \xi = 0.1$ and fractional orders $\alpha = 0.5, 0.8, 1$ respectively. In panel (a), the surface exhibits relatively periodic and regular high-frequency oscillations, indicating a system characterized by strong, coherent wave-like behavior with minimal damping. In panel (b), the oscillations remain evident but display increased irregularity and more pronounced troughs, suggesting a deviation from stability. Panel (c) presents the most chaotic and irregular oscillatory pattern, featuring deeper negative peaks and greater amplitude variation. Panel (d) presents a 2D plot at $x = 1$, with the same parameters. The figure illustrates the impact of varying the fractional order α on the time-dependent behavior of the system. As α decreases from 1 to 0.5, the oscillations exhibit reduced intensity and increased damping. In lower fractional orders result in smoother and broader waveforms.

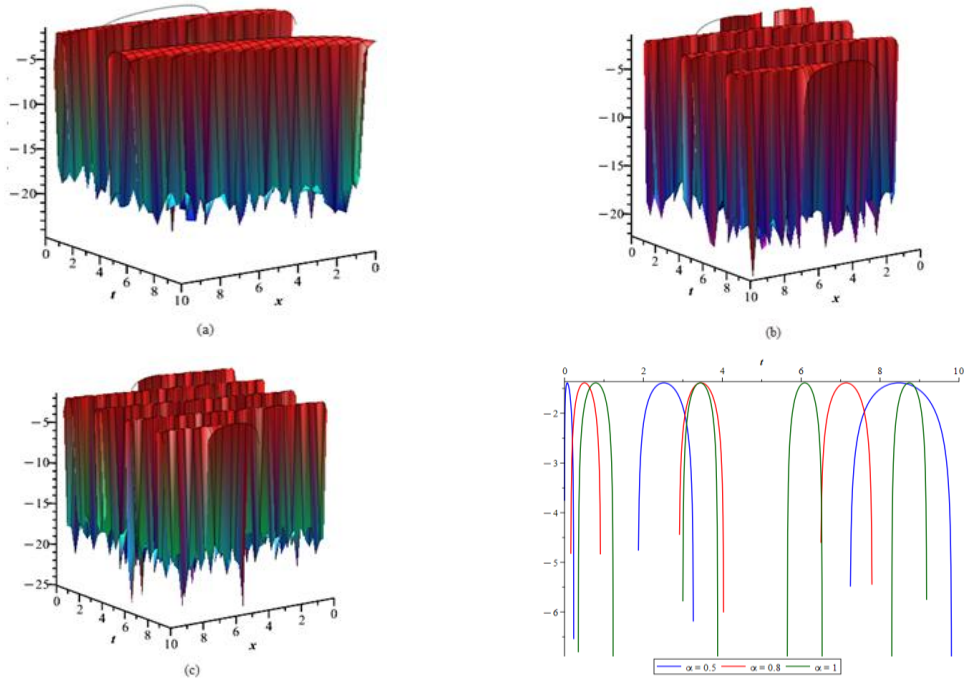

Figure.2. Behavior of periodic solutions: 3D and 2D visualizations of $w_{25}(x,t)$

Figure 3: Panels (a-c) depict 3D plots that present periodic solutions of $w_{26}(x,t)$ over the intervals $0 \le x,t \le 10$, with parameters $k = \eta_0 = 0.01, \beta = \gamma = 1, \xi = 0.001$ and fractional orders $\alpha = 0.5, 0.8, 1$ respectively. In panel (a), the solution exhibits sharp transitions along both the spatial and temporal axes, indicating strong discontinuities. Panel (b) displays smoother transitions with reduced amplitude. Panel (c) presents moderate sharpness and amplitude, representing an intermediate behavior that balances the characteristics observed in panels (a) and (b). Panel (d) presents 2D plots at $0.0007 \le t \le 0.002$, $x = 1$ with the same parameters. The plots highlight how fractional order influences early-time system behavior. While the $\alpha = 1$ case shows

smooth, classical dynamics, lower orders $\alpha = 0.5$ and $\alpha = 0.8$ result in sharp, high-frequency oscillations.

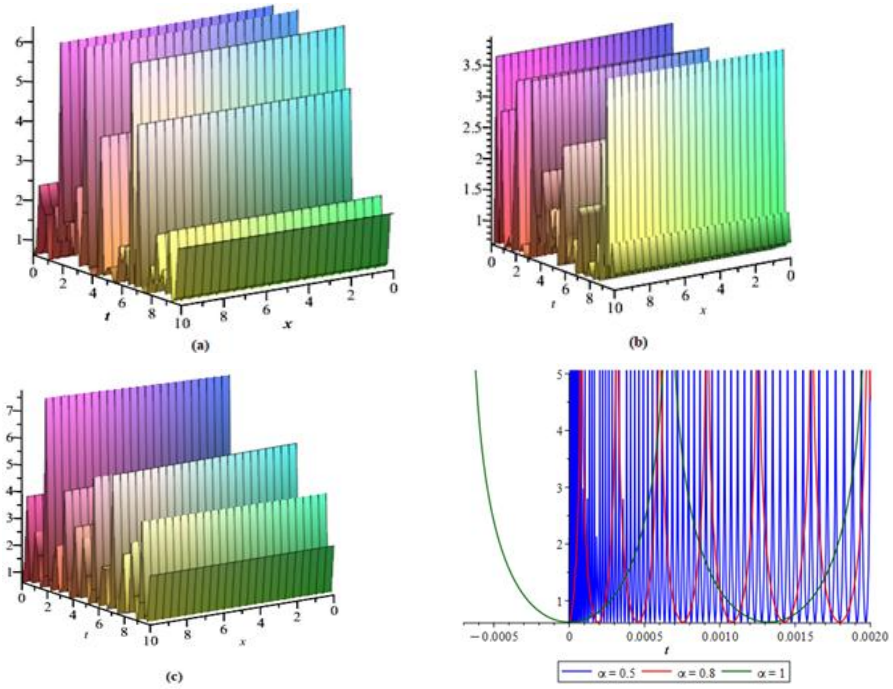

Figure 3. Behavior of periodic solution: 3D and 2D visualizations of $w_{26}(x,t)$.

Figure 4: Panels (a-b) depict 3D plots presenting shock soliton solutions, whereas panel (d) represents singular-dark soliton solutions of $w_{16}(x,t)$ over the intervals $-10 \le x \le 10$ and $0 \le t \le 10$, with parameters $k = 10$, $\eta_0 = 0$, $\xi = -100$ and fractional order $\alpha = 0.5, 0.8, 1$ respectively. The panels illustrate increasing spatial variability, with panel (a) showing a nearly flat surface, panel (b) presenting a sharper transition, and panel (c) demonstrating the most pronounced drop and curvature in the solution. Panel (d) presents 2D plots at the interval $-2 \le x \le 2$, $t = 1$ with the same parameters. All curves exhibit a sudden dip in a narrow region near $x = 0.5$. The sharpness and depth of this transition are influenced by the fractional order: the curve for $\alpha = 1$ shows the steepest and most pronounced drop. As α decreases to 0.8 and 0.5, the transition becomes less sharp and more spread out.

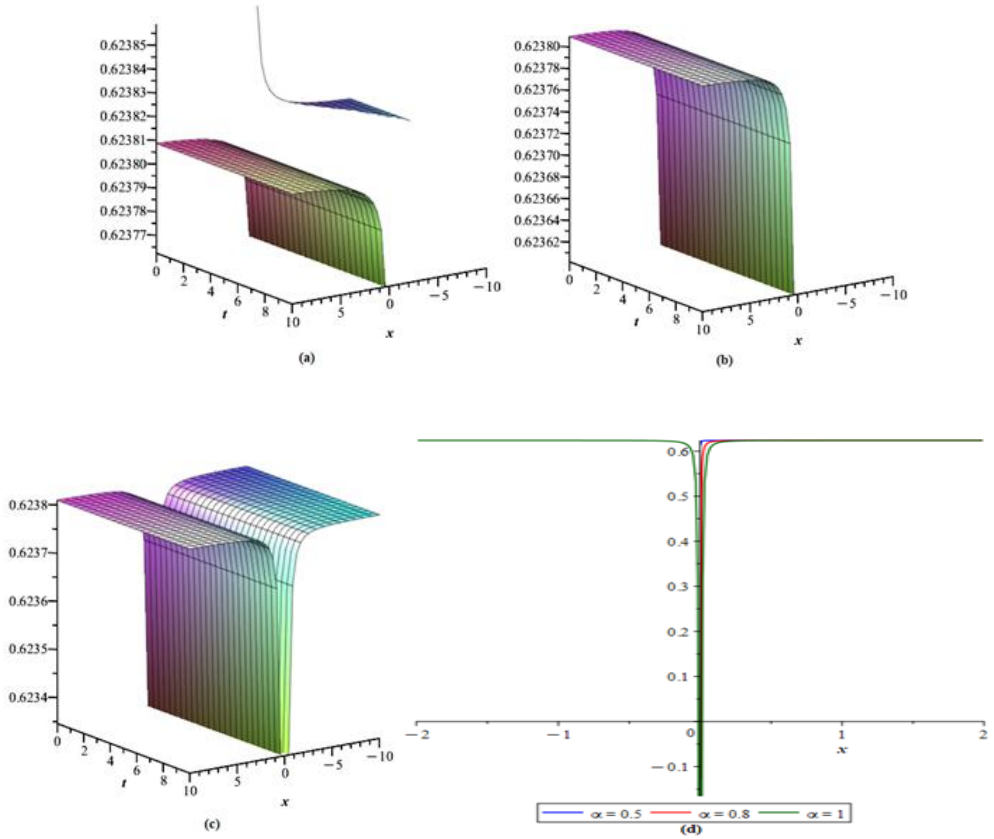

Figure 4. Behavior of wave soliton solution: 3D and 2D visualizations of $w_{16}(x,t)$.

5. Conclusions

The article applies the unified method to obtain exact solutions to the conformable fractional nonlinear Z-S equation. Several new exact solutions were derived, including hyperbolic, rational and periodic wave solutions. The 3D and 2D graphs were provided for some solutions to understand their physical behavior. All computations were performed using MAPLE software, highlighting the efficiency of the unified method in solving the Z–S equation. The results demonstrated the effectiveness of the unified method in solving NLFPDEs. The unified method can be extended to solve other classes of complex NLFPDEs.

Acknowledgements: The authors extend their appreciation to the Deanship of Scientific Research at Northern Border University, Arar, KSA for funding this research work through the project number "NBU-FFR-2025-2503-1.

Conflicts of Interest: The authors declare that there are no conflicts of interest regarding the publication of this paper.

References

[1] M. Wang, Y. Zhou, Z. Li, Application of a Homogeneous Balance Method to Exact Solutions of Nonlinear Equations in Mathematical Physics, Phys. Lett. 216 (1996), 67-75. https://doi.org/10.1016/0375-9601(96)00283-6.

[2] R. Hirota, The Direct Method in Soliton Theory, Cambridge University Press, Cambridge, 2004. https://doi.org/10.1017/CBO9780511543043.

[3] W. Malfliet, W. Hereman, The Tanh Method: I. Exact Solutions of Nonlinear Evolution and Wave Equations, Phys. Scr. 54 (1996), 563-568. https://doi.org/10.1088/0031-8949/54/6/003.

[4] M.J. Ablowitz, H. Segur, Solitons and Inverse Scattering Transform, SIAM, Philadelphia, 1981. https://doi.org/10.1137/1.9781611970883.

[5] M. Abdou, The Extended F-Expansion Method and Its Application for a Class of Nonlinear Evolution Equations, Chaos Solitons Fractals 31 (2007), 95-104. https://doi.org/10.1016/j.chaos.2005.09.030.

[6] J. He, X. Wu, Exp-function Method for Nonlinear Wave Equations, Chaos, Solitons Fractals 30 (2006), 700-708. https://doi.org/10.1016/j.chaos.2006.03.020.

[7] A. Hassaballa, M. Salih, G.S.M. Khamis, E. Gumma, A.M.A. Adam, A. Satty, Analytical Solutions of the Space–time Fractional Kadomtsev–Petviashvili Equation Using the (G′/G)-Expansion Method, Front. Appl. Math. Stat. 10 (2024), 1379937. https://doi.org/10.3389/fams.2024.1379937.

[8] N. Sharma, G. Alhawael, P. Goswami, S. Joshi, Variational Iteration Method for N-Dimensional Time-Fractional Navier–stokes Equation, Appl. Math. Sci. Eng. 32 (2024), 1–12. https://doi.org/10.1080/27690911.2024.2334387.

[9] Z. Odibat, An Optimized Decomposition Method for Nonlinear Ordinary and Partial Differential Equations, Physica A: Stat. Mech. Appl. 541 (2020), 123323. https://doi.org/10.1016/j.physa.2019.123323.

[10] J. Sabatier, O.P. Agrawal, J.A.T. Machado, Advances in Fractional Calculus, Springer Netherlands, Dordrecht, 2007. https://doi.org/10.1007/978-1-4020-6042-7.

[11] H. Sun, Y. Zhang, D. Baleanu, W. Chen, Y. Chen, A New Collection of Real World Applications of Fractional Calculus in Science and Engineering, Commun. Nonlinear Sci. Numer. Simul. 64 (2018), 213--231. https://doi.org/10.1016/j.cnsns.2018.04.019.

[12] R. Hilfer, Applications of Fractional Calculus in Physics, World Scientific, Singapore, 2000. https://doi.org/10.1142/3779.

[13] A.A. Kilbas, H.M. Srivastava, J.J. Trujillo, Theory and Applications of Fractional Differential Equations, Elsevier, 2006. https://doi.org/10.1016/s0304-0208(06)x8001-5.

[14] A. Wazwaz, The Tanh Method for Travelling Wave Solutions to the Zhiber–Shabat Equation and Other Related Equations, Commun. Nonlinear Sci. Numer. Simul. 13 (2008), 584-592. https://doi.org/10.1016/j.cnsns.2006.06.014.

[15] Y. Tang, W. Xu, J. Shen, L. Gao, Bifurcations of Traveling Wave Solutions for Zhiber–Shabat Equation, Nonlinear Anal.: Theory Methods Appl. 67 (2007), 648-656. https://doi.org/10.1016/j.na.2006.06.024.

[16] H.A. Ghany, A. Fathallah, Exact Solutions for Stochastic Fractional Zhiber-Shabat Equations, J. Comput. Anal. Appl. 29 (2021), 634–644.

[17] M.G. Hafez, M.A. Kauser, M.T. Akter, Some New Exact Traveling Wave Solutions for the Zhiber-Shabat Equation, Br. J. Math. Comput. Sci. 4 (2014), 2582-2593. https://doi.org/10.9734/bjmcs/2014/11563.

[18] M. Inc, New Type Soliton Solutions for the Zhiber–Shabat and Related Equations, Optik 138 (2017), 1-7. https://doi.org/10.1016/j.ijleo.2017.02.103.

[19] A. Yokus, H. Durur, H. Ahmad, S. Yao, Construction of Different Types Analytic Solutions for the Zhiber-Shabat Equation, Mathematics 8 (2020), 908. https://doi.org/10.3390/math8060908.

[20] Y. Ding, B. He, W. Li, A Improved F-expansion Method and Its Application to the Zhiber–Shabat Equation, Math. Methods Appl. Sci. 35 (2012), 466-473. https://doi.org/10.1002/mma.1574.

[21] A.G. Davodi, D.D. Ganji, Travelling Wave Solutions to the Zhiber-Shabat and Related Equations Using Rational Hyperbolic Method, Adv. Appl. Math. Mech. 2 (2010), 118-130. https://doi.org/10.4208/aamm.09-m0939.

[22] A. Borhanifar, A.Z. Moghanlu, Application of the (G′/G)-Expansion Method for the Zhiber–Shabat Equation and Other Related Equations, Math. Comput. Model. 54 (2011), 2109-2116. https://doi.org/10.1016/j.mcm.2011.05.020.

[23] L. Wazzan, Solutions of Zhiber-Shabat and Related Equations Using a Modified Tanh-Coth Function Method, J. Appl. Math. Phys. 04 (2016), 1068-1079. https://doi.org/10.4236/jamp.2016.46111.

[24] A.R. Butt, N. Akram, A. Jhangeer, M. Inc, Propagation of Novel Traveling Wave Envelopes of Zhiber–Shabat Equation by Using Lie Analysis, Int. J. Geom. Methods Mod. Phys. 20 (2023), 2350091. https://doi.org/10.1142/s0219887823500913.

[25] R.K. Alhefthi, K.U. Tariq, A. Bekir, A. Ahmed, On Some Novel Solitonic Structures for the Zhiber–Shabat Model in Modern Physics, Z. Naturforsch. A 79 (2024), 643-657. https://doi.org/10.1515/zna-2024-0010.

[26] M.W. Yasin, M.Z. Baber, A. Butt, I. Saeed, T.A. Sulaiman, A. Yusuf, M. Bayram, S. Salahshour, Visualization of the Impact of Noise of the Closed-form Solitary Wave Solutions for the Stochastic Zhiber–Shabat Model, Mod. Phys. Lett. A 40 (2025), 2550077. https://doi.org/10.1142/S0217732325500774.

[27] K.S. Miller, B. Ross, An Introduction to the Fractional Calculus and Fractional Differential Equations, John Wiley & Sons, New York, 1993.

[28] I. Podlubny, Fractional Differential Equations, Academic Press, London, 1999.

[29] A. Atangana, E.F.D. Goufo, Extension of Matched Asymptotic Method to Fractional Boundary Layers Problems, Math. Probl. Eng. 2014 (2014), 107535. https://doi.org/10.1155/2014/107535.

[30] R. Khalil, M. Al Horani, A. Yousef, M. Sababheh, A New Definition of Fractional Derivative, J. Comput. Appl. Math. 264 (2014), 65-70. https://doi.org/10.1016/j.cam.2014.01.002.

[31] Z. Al-Zhour, N. Al-Mutairi, F. Alrawajeh, R. Alkhasawneh, New Theoretical Results and Applications on Conformable Fractional Natural Transform, Ain Shams Eng. J. 12 (2021), 927-933. https://doi.org/10.1016/j.asej.2020.07.006.

[32] T. Aydemir, Traveling-wave Solution of the Tzitzéica-Type Equations by Using the Unified Method, Theor. Math. Phys. 216 (2023), 944-960. https://doi.org/10.1134/s0040577923070048.

[33] S. Akcagil, T. Aydemir, A New Application of the Unified Method, New Trends Math. Sci. 1 (2018), 185-199. https://doi.org/10.20852/ntmsci.2018.261.

[34] N. Alam, M.S. Ullah, T.A. Nofal, H.M. Ahmed, K.K. Ahmed, M.A. AL-Nahhas, Novel Dynamics of the Fractional KFG Equation Through the Unified and Unified Solver Schemes with Stability and Multistability Analysis, Nonlinear Eng. 13 (2024), 20240034. https://doi.org/10.1515/nleng-2024-0034.

[35] F. Bekhouche, M. Alquran, I. Komashynska, Explicit Rational Solutions for Time-Space Fractional Nonlinear Equation Describing the Propagation of Bidirectional Waves in Low-Pass Electrical Lines, Rom. J. Phys. 66 (2021), 114.

[36] M.S. Ullah, A. Abdeljabbar, H. Roshid, M.Z. Ali, Application of the Unified Method to Solve the Biswas–arshed Model, Results Phys. 42 (2022), 105946. https://doi.org/10.1016/j.rinp.2022.105946.

[37] F. Bekhouche, I. Komashynska, Traveling Wave Solutions for the Space-Time Fractional (2+1)-Dimensional Calogero–Bogoyavlenskii–Schiff Equation via Two Different Methods, Int. J. Math. Comput. Sci. 16 (2021), 1729–1744.